IOP Publishing Plasma Sources Science and Technology

Plasma Sources Sci. Technol. **24** (2015) 035021 (10pp) doi:10.1088/0963-0252/24/3/035021

Gas purification by the plasma-oxidation of a rotating sacrificial electrode

S Dahle[1,2], J Hirschberg[3,4], W Viöl[3,4] and W Maus-Friedrichs[1,2]

[1] Clausthaler Zentrum für Materialtechnik, Technische Universität Clausthal, Leibnizstr. 4, 38678 Clausthal-Zellerfeld, Germany
[2] Institut für Energieforschung und Physikalische Technologien, Technische Universität Clausthal, Leibnizstr. 4, D-38678 Clausthal-Zellerfeld, Germany
[3] Department of Science and Technology, HAWK University of Applied Sciences and Arts, Von-Ossietzky-Str. 99, 37085 Göttingen, Germany
[4] Fraunhofer Institute for Surface Engineering and Thin Films IST, Application Center for Plasma and Photonic APP, Von-Ossietzky-Str. 100, 37085 Göttingen, Germany

E-mail: s.dahle@pe.tu-clausthal.de

Received 16 December 2014, revised 19 April 2015
Accepted for publication 14 May 2015
Published 2 June 2015

Abstract

A novel approach for the purification of inert gases by means of a dielectric barrier discharge (DBD) plasma has been demonstrated for argon and nitrogen. A rotating sacrificial electrode has been employed together with an electrode cleaning system to remove passivating product films during the plasma processing and thus enhance capacity and reaction rates. The purification of nitrogen using this approach was shown to be quite successful. The conditioning of technical argon yielded rotational temperatures well beyond 150 °C, thus being unable to remove the water content effectively.

Keywords: DBD, argon, nitrogen, gas purification

(Some figures may appear in colour only in the online journal)

1. Introduction

The plasma treatment of workpieces is strongly affected by the composition of the gases used to ignite a plasma discharge. In many cases even small amounts of gaseous impurities can drastically change the impact of the plasma processing on the chemistry and the structure of the treated surface. During the plasma treatment of titanium metal foils in nitrogen for example, the use of technical nitrogen (Linde Gas, 99.8%) yielded the formation of a stoichiometric TiO_2 film with a thickness much larger than 10 nm and a nitrogen content of less than 1.5% (Dahle *et al* 2012). While titanium oxide is slightly more favorable than titanium nitride regarding thermodynamic binding enthalpies (cf Lide 1998), the concentration of oxygen molecules is much smaller than the concentration of nitrogen molecules. Thus, a significant rate of the backwards reaction i.e. the nitride formation would be assumed according the law of mass action (cf Guldberg and Waage 1879). This is obviously not the case, but by the use of the plasma process it is possible to yield almost only the thermodynamic most favorable chemical state. As such, the preferred gas species during the reaction is selectively removed from the gas. Hence, the plasma treatment of cheap workpieces might be used for gas purification purposes.

The purification of nitrogen and noble gases requires huge amounts of energy when using present techniques and processes.

Nitrogen for example is purified by liquefaction, using solid or liquid absorber, or membranes. The processes using the liquefaction of nitrogen-containing gases typically require high pressures and low temperatures (DeMarco 1967, Yao *et al* 1986, Kamrath 1990, Bergman *et al* 1999, Greter and Venet 2003). The solid absorber processes utilize expensive materials at high temperatures (Newton 1949, Gajula *et al* 2009) and have to be regenerated (Jain 1994, Hsiung and Wallace 1999) or replaced quite often, while liquid absorber processes usually employ high pressures (Reich and Kapenekas 1957). Membrane-based purification also requires high temperatures (Campbell 1990, Lawless 2001). In many cases, combinations of these approaches are used (Campbell 1990, Kamrath 1990).

Thus, all current processes for the purification of nitrogen require huge amounts of energy.

Noble gases are produced using spongy transition metal structures at high temperatures (Koichi *et al* 1997) and high pressures (Takao *et al* 1969), using membranes at very low temperatures (Bligh and Godber 1980), by nitrogen washing at very low temperatures and high pressures (Bauer *et al* 1988), or by a combination of several of such purification devices (Mallett 1950, Jain and Tseng 1998, Yamamoto and Yamashita 2001).

Especially some of the processes employing catalysts or diffusion devices are applicable for the purification of several different gases (Boveri *et al* 1995, Baker *et al* 1997, Lane *et al* 2009). All of these processes need at least one of the extensive thermodynamic state variables pressure and temperature to be strongly varied, thus they require large amounts of mechanical energy to realize the pressures and temperatures needed. Many of these processes even require huge variations of both, pressure and temperature, which is particularly obvious for freezing process as used in a cryo trap. In this way, however, the mechanical energy is used in a very indirect way to achieve changes of molecular dynamics or reaction kinetics. For example, the typical reason to operate purification processes at high temperatures is to increase either the diffusion lengths within the absorber material or the reaction rates of the residual gas contents during chemisorption. Both tasks can also be achieved by plasma discharges through the dissociation of the residual gas contents and the generation of highly reactive species. In this way, the energy is transferred mainly into the mean energy of the valence electrons mediating the chemical bonds, hence being able to probably save huge amounts of energy.

Nevertheless, no plasma-based processes for the purification of nitrogen, hydrogen or noble gases have been reported up to now. However, the plasma treatment of various substrates under inert gases has been found to mainly result in an oxidation of the substrate (Dahle *et al* 2012). This might be due to intermolecular energy transfer processes within the plasma (Penetrante *et al* 1997). Furthermore, it is possible to convert nitrides into oxides by means of plasma discharges under oxygen-containing atmospheres, even in the case of rather low oxygen contents (Dahle *et al* 2013). During the plasma treatment of substrates, highly selective processes like the above-mentioned can be assumed to have an impact on the composition of the process gas, too. For this application, the highly reactive species produced in the plasma will significantly improve the absorption rates in comparison to ordinary sorbents, while the adsorption takes place as a chemical reaction rather than a pure physisorption and should thus be much more stable. Furthermore, this kind of plasma-driven chemisorption, i.e. oxidation or corrosion would be superior to a simple adsorption filter because of the significantly enhanced penetration depths, which exceed the thickness of any natural passivation layer by far as illustrated below in section 2. Additionally, this plasma-based process could have an influence on all contaminants found within the gas, while some of the currently used processes are quite selective. For example, the use of a cryo trap would significantly reduce the water content, while the oxygen partial pressure should remain largely unaffected. Moreover, the adsorption of the water vapor on the cryo trap would be reversible unlike the proposed plasma-based process, which should also be energetically favorable over the cryo trap. In this study, first results on the impacts of the process gas composition during the plasma oxidation of a simple metal target are presented.

2. Experimental

The ideal material for a metal target used as sacrificial electrode should cheap and easy available. On one hand, it should exhibit a large capacity for all gaseous contaminants that shall be removed, i.e. mainly oxygen, water and carbon oxides. On the other hand, the volume difference between the clean and the loaded state should be as large as possible, since this leads to mechanical stress and brittle fracturing, thus exposing unloaded electrode material to the gas stream. A very good example for this mechanism is the atmospheric corrosion of iron workpieces. Each square centimeter of an iron surface holds 1.9×10^{15} atoms per surface layer, while there are about 2.5×10^{19} atoms per cubic centimeter of ambient air at atmospheric pressure. Thus, the specific adsorbation capacity of an iron electrode calculates to 76 ppm·cm^3 of gaseous contaminants per atomic layer at 1 cm^2 surface area. Even though the plasma discharge is able to oxidize metal as deep as several dozen nanometers, this is not sufficient to remove high concentrations of contaminants from the gas. Therefore, we used a rotating electrode at a rotational speed of 4 rpm together with a brush as cleaning device. Hollow steel cylinders (AISI 304, outer diameter 14 mm, inner diameter 10 mm, length 35 mm) have been used as sacrificial electrode to reduce the effects of atmospheric corrosion and to investigate the sole use of plasma-driven interactions. Figure 1(a) displays these sacrificial electrodes before (left) and after plasma processing for about 5 h (right). The electrode exhibits significant effects of oxidation with a penetration depth in the order of magnitude of 0.1 mm on stainless steel (AISI 304), while typical corrosion rates even for cast iron stored in aqueous salt solution would only be in the order of magnitude of 0.02 mm per year (El-Mahdy *et al* 2012), thus illustrating the high reaction rates and penetration depths due to the plasma-enhanced chemisorption during the treatment process. Figure 1(b) show a 3D sketch of the used plasma setup within the reaction chamber used as vessel (see below), while the other attached equipment is not shown to clarify the presentation of the plasma setup. A partial cutaway view at the front corner reveals the 3D sight of the sacrificial electrode fitted to a standard UHV linear-rotary mechanical feedthrough. The sacrificial electrode is placed between the brush as cleaning device at the back on the left side and the dielectrically isolated HV electrode at the front on the right side. The blue box contains a detailed view onto the described setup parallel to the rotational axis of the sacrificial electrode with the brush being in contact on its left side and the isolated HV electrode at a working distance of 1 mm on the sacrificial electrode's right side. For details on the isolated HV electrode confer Wegewitz *et al* (2011). Figures 1(c)

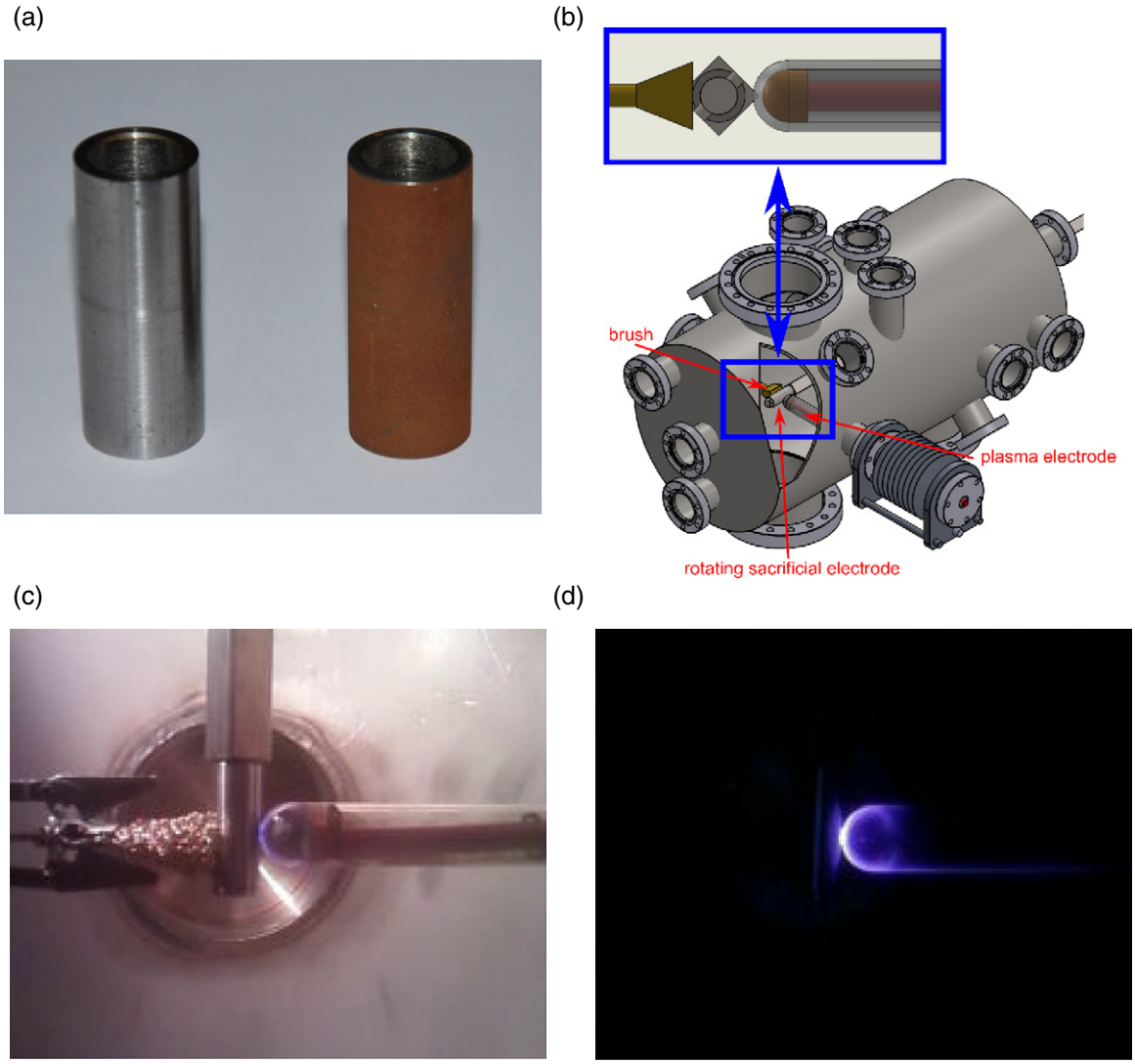

Figure 1. (a) Picture of the used sacrificial electrodes before (left) and after (right) plasma processing for about 5 h, (b) simplified CAD sketch of the plasma setup, (c) top view image of the plasma setup taken through the top viewport and (d) top view image of the setup during plasma processing of Ar at 1000 mbar.

and (d) contain photographs of the setup during plasma processing of an argon atmosphere at 1000 mbar with (c) and without illumination of the vessel via a built-in light bulb (d).

The plasma discharge was ignited as a dielectric barrier discharge, applying alternating high voltage pulses with a pulse duration of 0.6 μs and a pulse repetition rate of 1.7 kHz at the dielectric isolated electrode, while the sacrificial counter electrode remained at ground potential. The discharge gap is set to about 1 mm and the discharge area is about 2 cm^2. During the plasma treatment, a voltage of 11 kV (peak) is measured. The high voltage supply delivers a power of 2 W, the plasma power density can be calculated to 1 W cm^{-2} (cf Avramidis *et al* 2012).

The plasma setup was placed inside a stainless steel reaction vessel with a volume of approx. 25 dm^3. The chamber can be evacuated by a commercial rotary vane pump (Pfeiffer DUO 5 M) and a turbomolecular pump (Pfeiffer TMH 250) and can be operated at pressures of several 10^{-10} mbar up to 1000 mbar. A bakeable leak valve as well as a gate valve lead into a analytical UHV chamber which is equipped with a quadrupole mass spectrometer (Balzers QMS 112A), thus being able to analyze gas compositions within the reaction chamber over the whole range of operating pressures. For the quantitative analysis of the mass spectra, relative sensitivity factors and fragmentation intensities were taken into account. A gas inlet system attached via a bakeable leak valve was used to fill the reaction chamber with argon (Linde Gas, 99.999 %) or N_2 (Linde Gas, 99.8%), respectively. The gas line was evacuated prior to the experiments, but no bake-out procedure was performed.

The rotational and vibrational as well as the electron temperatures during plasma processing were determined by optical emission spectroscopy (OES) using the commercial Echelle spectrometer Aryelle-Butterfly 400 (LTB Lasertechnik Berlin GmbH, Berlin, Germany). The rotational temperatures have been evaluated regarding the rotational lines of the 0-0 vibrational band in the second positive system of nitrogen at 337.1 nm (Fantz 2006, Staak *et al* 2005). The simulation program SpecAir (Laux 2002) was used for modelling emission spectra. By comparing

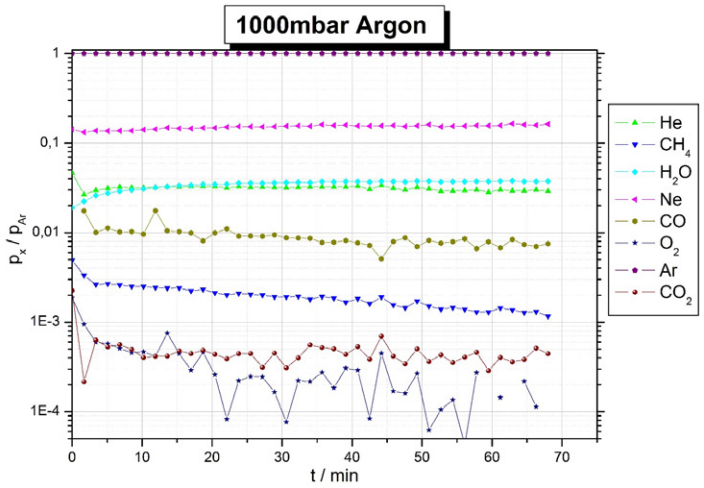

Figure 2. Progression of the QMS intensity relative to argon for the main gas species within a 1000 mbar argon atmosphere during plasma treatment.

simulated with experimental spectra, the rotational temperature was determined applying the least squares method. To identify the vibrational temperatures, the intensity ratios of the 0-1 vibrational transition at 357.6 nm and the 1–2 vibrational transition at 337.1 nm in the N_2 second positive system in simulated and experimental spectra were compared. Error values for rotational and vibrational temperatures have been calculated after Laux (2003).

The electron temperatures have been determined from the intensity ratios between the nitrogen emissions lines at 391.4 nm (0-0 vibrational band, first negative system) and 337.1 nm (0-0 vibrational band, second positive system) by the evaluation procedure after Paris *et al* (2005). The dependence of intensity ratios from reduced electric field strength and hence from the mean electron energy was appropriated for the process gases N_2 and ambient air. For this purpose, the BOLSIG+ software (Hagelaar and Pitchford 2005) was used to obtain the electron energy distribution function from the solution of the Boltzmann equation for electrons in weakly ionized gases. (q.v. Hirschberg *et al* 2013)

3. Results

The plasma treatment of all gases has been investigated at two different pressures, i.e. atmospheric pressure as well as low pressures. Thus, a pressure dependence on the reaction rates and process has can be evaluated. However, the pressures have been chosen high enough to avoid a change of the plasma conditions from a strongly localized plasma volume and a high density of filaments towards the distribution of the plasma throughout the whole reaction chamber with a low density of filaments. The electrode cleaning device was used during all experiments with the sole exception being the 200 mbar Ar atmosphere, as described in detail later on.

Figure 2 shows the progression of the main gas species within a 1000 mbar argon atmosphere over plasma treatment time, all partial pressures have been scaled relative to argon. The typical impurities found within argon are lighter noble gases, i.e. neon and helium. Both show a dip in intensity during the first 5 min of plasma treatment. The partial pressure of water relative to argon increased from 0.02 to 0.04 during the 60 min of plasma conditioning. The other contaminants were CO, CO_2 and O_2. They decreased by a factor of 2.4, 5.9 and 8.6, respectively. The gas compositions before and after the plasma conditioning from all experiments have been summarized in table 1.

Figure 3 depicts the progression during the conditioning of an argon atmosphere at 100 mbar. The lighter noble gas impurities remained unaffected, again, after a first transient phase of about 10 min. The nitrogen fraction decayed from 0.2 down below the detection limits, while water, CO and CO_2 remained nearly unaffected after the first 10 min of conditioning. The relative partial pressure of methane had a maximum of 0.005 after 10 min of plasma treatment, but afterwards decayed down to the initial content well below 0.001. This might indicate a transient phase of CH_4 production. The oxygen content decayed rapidly and dropped below the detection limit after just 10 min.

To draw a comparison between the experiments described above and a gas conditioning without removing the passivation layer, the cleaning device was disable during the next experiment. Thus, an additional dielectric film was formed upon the grounded electrode during the course of the plasma conditioning. This was taken into account by the application of a slightly raised pressure to stay within the given plasma regime, while the particle density and thus rate of formation of the passivation layer was still significantly lower than for an atmospheric pressure discharge. Figure 4 exhibits the progression during the conditioning of an argon atmosphere at 200 mbar with a fixed electrode. During this experiment, no transient phase took place at the beginning of the plasma treatment. The noble gas species were present, but unaffected by the conditioning, again. Under these circumstances, a constant reduction was found for CO, N_2, O_2 and CO_2, removing over 90% of all of these species within 40 min. The partial pressures of water and methane however remained mainly unaffected.

Table 1. Gas compositions for argon, nitrogen and air atmospheres before and after plasma conditioning.

Gas	Pressure	Brush	Plasma	He	CH_4	H_2O	N_2	CO	O_2	Ar	CO_2
Argon	200 mbar	No	Before	0.8%	0.2%	3.0%	8.9%	17.6%	8.5%	59.7%	1.4%
			After	3.4%	0.3%	4.3%	1.3%	1.0%	0.3%	89.4%	0.1%
Argon	100 mbar	Yes	Before	0.0%	0.1%	1.2%	11.0%	0.5%	0.1%	87.1%	0.0%
			After	0.1%	0.1%	3.4%	0.0%	0.7%	0.0%	95.7%	0.0%
Argon	1000 mbar	Yes	Before	4.2%	0.4%	1.7%	2.1%	0.0%	0.2%	91.1%	0.2%
			After	2.7%	0.1%	3.5%	0.0%	0.7%	0.0%	93.0%	0.0%
Nitrogen	100 mbar	Yes	Before	0.2%	0.0%	1.3%	91.5%	0.0%	0.2%	6.8%	0.0%
			After	0.1%	0.0%	0.4%	96.8%	0.0%	0.0%	2.6%	0.0%
Nitrogen	1000 mbar	Yes	Before	0.3%	0.0%	1.2%	92.5%	0.0%	0.0%	5.9%	0.0%
			After	0.0%	0.0%	0.7%	96.5%	0.0%	0.0%	2.7%	0.0%
Air	100 mbar	Yes	Before	0.1%	0.0%	1.2%	86.6%	0.0%	8.9%	3.1%	0.0%
			After	0.1%	0.0%	1.0%	87.2%	0.0%	9.0%	2.7%	0.1%
Air	1000 mbar	Yes	Before	0.3%	0.1%	1.4%	85.5%	0.0%	9.4%	3.3%	0.1%
			After	0.2%	0.0%	1.1%	86.2%	0.0%	9.5%	2.8%	0.1%

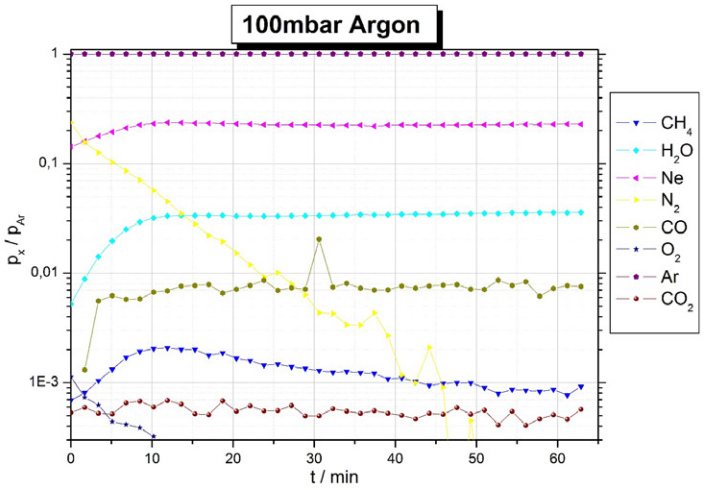

Figure 3. Progression of the QMS intensity relative to argon for the main gas species within a 100 mbar argon atmosphere during plasma treatment.

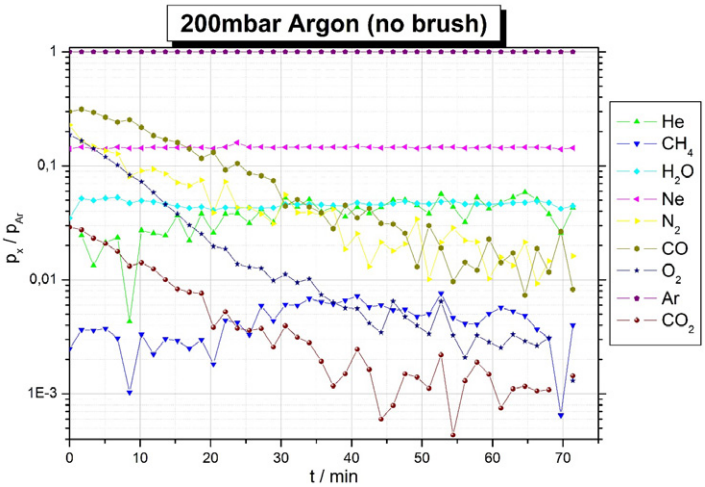

Figure 4. Progression of the QMS intensity relative to argon for the main gas species within a 200 mbar argon atmosphere during plasma treatment without cleaning.

Afterwards, the process gas was changed from a noble gas to technical nitrogen as typical inert cover gas. During all of the following experiments, the electrode cleaning device was used, thus removing the passivation film formed during the gas conditioning process. Figure 5 shows the progression during the conditioning of a nitrogen atmosphere at

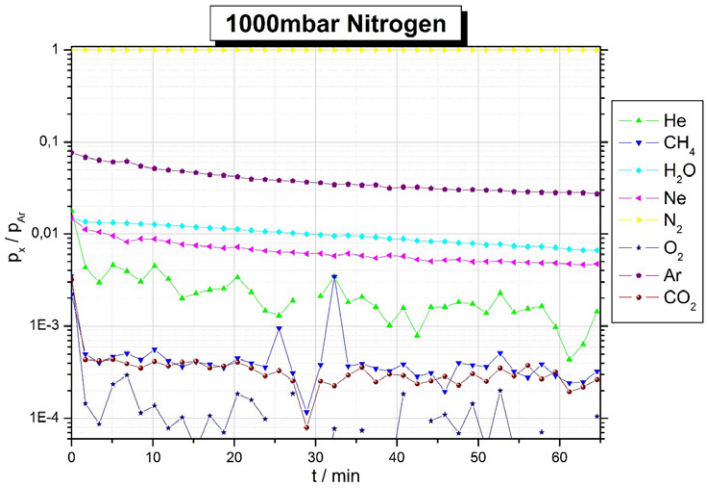

Figure 5. Progression of the QMS intensity relative to nitrogen for the main gas species within a 1000 mbar nitrogen atmosphere during plasma treatment.

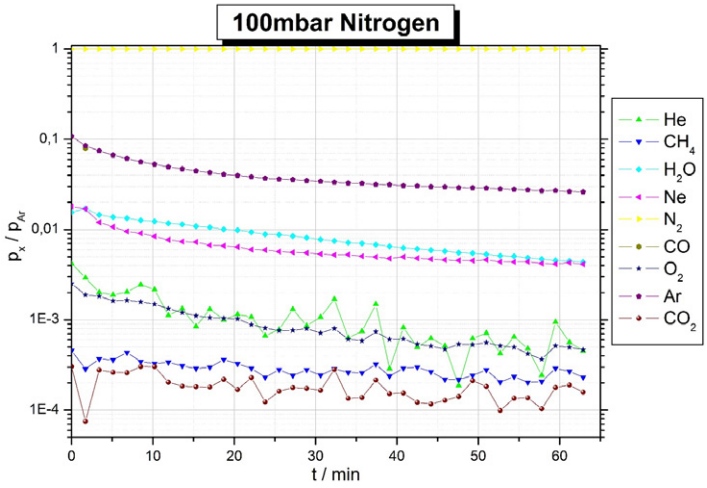

Figure 6. Progression of the QMS intensity relative to nitrogen for the main gas species within a 100 mbar nitrogen atmosphere during plasma treatment.

1000 mbar. The initial content of water, oxygen, CO_2 and CH_4 decreased very quickly during first 3 min of plasma treatment. However, all gas species decayed slowly during the whole time of gas conditioning. The effect of the plasma procedure on a nitrogen atmosphere at 100 mbar was qualitatively the same, as depicted in figure 6.

The progression of the main gas species during the conditioning of ambient air at 1000 mbar and 100 mbar (not shown) yielded a negligible effect of the plasma treatment for all gas species. The components intended to be removed from ambient air were the same as for nitrogen and argon atmospheres, i.e. mainly oxygen, water and carbon oxides. The complete removal of these contaminants was unlikely from the beginning as indicated by the discussion of the possible chemisorption capacities (cf section 2). Nevertheless, the aim was maybe to be able to gain some insight in the reaction processes, in case the reaction rates would significantly differ from those identified for the nitrogen atmospheres. However, the removal rates for the conditioning of ambient air were even smaller than expected.

The measurement of the translational and rotational temperatures as well as the electron temperature was done in a different, smaller chamber to fit into the analytical device. Therefore, no electrode rotation and thus no removal of the passivation layer took place, while the same sacrificial and high voltage electrodes were used as during the mass spectrometry measurements. To be able to apply low pressures and clean gas atmospheres without contact to ambient air, a UV-transparent window separated the reaction chamber and the spectrometer. The transmission function of the window was determined and the data corrected accordingly prior to quantitative analysis.

Figure 7 exemplarily shows one measured spectrum and the simulated best fit of the 0-0 vibrational transition of the second positive system of nitrogen including the rotational bands. For the calculation of the mean rotational temperature the wavelength range from 334 nm up to 337 nm was used. The accuracy of this method is about 50 K for rotational as well as vibrational temperatures (Laux 2003). The resulting rotational temperatures were in the 305–465 K range, the vibrational

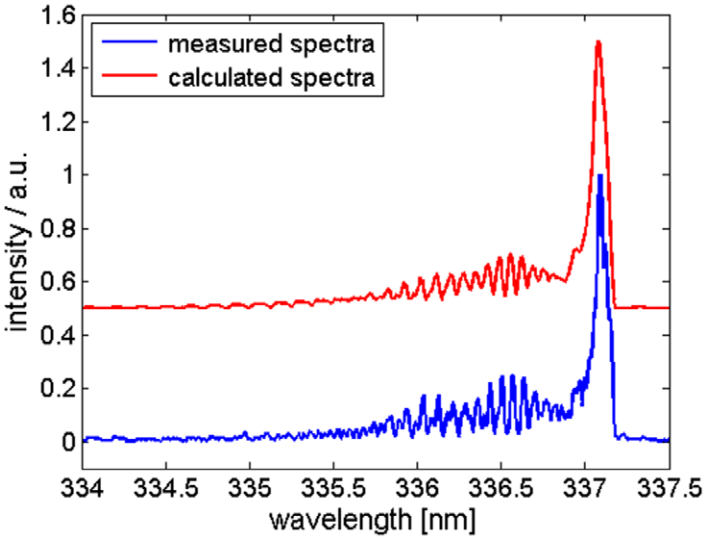

Figure 7. Optical emission spectrum (blue line) as well as the simulation (red line) for a plasma discharge in 1000 mbar of argon.

Table 2. Rotational, vibrational and electron temperatures as well as reduced electric fields as calculated from OES measurements.

Gas	Pressure	T_{rot}	T_{vib}	T_e/ε	E/N
Argon	100 mbar	465 K	2500 K	—	—
Argon	1000 mbar	450 K	2200 K	—	—
Nitrogen	100 mbar	385 K	2300 K	5.195×10^4 K / 6.7 ± 1.0 eV	300 Td
Nitrogen	1000 mbar	365 K	2250 K	5.805×10^4 K / 7.5 ± 1.1 eV	360 Td
Air	100 mbar	360 K	1700 K	5.560×10^4 K / 7.2 ± 1.1 eV	290 Td
Air	1000 mbar	305 K	1550 K	6.554×10^4 K / 8.5 ± 1.3 eV	370 Td

temperatures are about 1550 K up to 2500 K. The highest rotational temperatures were measured in the Ar-discharge, the plasma-discharge in ambient air exhibits the lowest values. The discharges always show higher rotational temperatures in vacuum, compared to atmospheric pressure. This behavior could be explained by the lower collision frequency in vacuum and the resulting decrease in energy transfer. The determined electron temperatures are in a range of 5.2×10^4 K to 6.6×10^4 K (6.7 eV – 8.5 eV), including higher temperatures at normal pressure for both regarded plasma discharges. The values of the mean electron energy might appear relatively high, however, they are comparable to the results for similar setups found in the literature (cf Hirschberg *et al* 2013). The entire temperatures calculated as well as an error range according to Paris *et al* (2005) and the corresponding reduced electric fields are listed in table 2.

4. Discussion

The results reveal quite different behaviors for argon, nitrogen and air during the plasma conditioning process. At high contents of contaminants, the rates of the chemisorption at the sacrificial electrode are insufficient. For example, the purification of nitrogen from air, i.e. a nitrogen gas mixture with a content of approx. 20% oxygen as main contaminant amongst others, would require an oxidation depth at the sacrificial electrode in the order of magnitude of 1 mm for the given setup. This possible problem about the oxidation depth of the sacrificial electrode is very well represented by the only slightly decreased water content within the gas air atmosphere, while especially the oxygen content remained constant. The gas composition, however, is distinctly influenced by different plasma-chemical reactions, i.e. a decrease of the water content by one-fifth and a decrease of the carbon monoxide content by about 50%. The hydrogen content within the gas and its variation due to the plasma processing has not been addressed during this study. Since one of the pumps attached to the analysis chamber tends to release hydrogen at high pressures of inert gases, the recorded development of the hydrogen partial pressures might differ from the hydrogen partial pressure within the working gas. Hence, the authors did not specify the determined hydrogen (H and H_2) partial pressures (cf table 1).

The results for the treatment of nitrogen by the DBD plasma setup reveal a reduction of all gaseous contaminants. The rates, however, are rather small. Especially the disappearance of argon was not expected and the underlying mechanisms are not yet clear, even though the effect turned out to be reproducible. A prospective study on the fundamental processes at the interface between sorbent and adfilm may be able to clear out this effect. After more than one hour of plasma conditioning, the nitrogen content raised from 91.5 to 96.8% at 100 mbar and from 92.5 to 96.5% at 1000 mbar. The overall reduction of all other gas components calculates to 62 and 53% for 100 mbar and for 1000 mbar, respectively. Even though these reaction

rates are much higher than the rates of atmospheric corrosion, the reaction is still too slow to be used for most of the possible applications. Since the volume of the plasma discharge comprises just 1/10 000th of the setup's overall volume, an involvement of the whole gas volume and an increased surface-volume-ration might render the application of a plasma-based gas purification method possible. Especially the use of a fine powder sorbent within a plasma setup featuring large electrode areas might be reasonable towards a purification of medium quality inert gases.

The conditioning of argon did significantly reduce the main contaminants nitrogen and oxygen. Even though iron oxides are thermodynamically preferable in comparison to iron nitrides or oxynitrides, both gas species are effectively reduced. The main reasons for this unlikely behavior might be the Penning excitation of N and the Penning dissociation of N_2 due to Ar metastables, both leading to a strongly increasing electron density and a slightly decreasing electron temperature (Song *et al* 2011) as well as increased values and a surplus distinct high-energy component within the electron energy distribution function (cf Schah *et al* 2009). The presence of significant water contents, however, represents a big issue for the purification of argon by the presented setup. In contrast to all other gas components, the water content significantly increases during the plasma treatment of the argon atmospheres. This might be induced by the increased rotational and vibrational temperatures during the plasma conditioning of argon atmospheres, which might deliver sufficient energy to split hydrates of iron oxides and thus release water molecules that were stably chemisorbed in the cases of the nitrogen and air plasma discharges. The main component of the stainless steel used as sacrificial electrode is iron, which is at least partly converted into the oxide state. Iron oxides are known to form γ-FeO(OH) and even further take up water (Rodt 1930) via

$$Fe_2O_3 + 2H_2O \rightarrow 2FeO(OH), \quad (1)$$

$$FeO(OH) + n\,H_2O \rightarrow FeO(OH) \cdot nH_2O. \quad (2)$$

The decomposition temperatures of these hydrates depends strongly on the number of water molecules per iron ion incorporated into the hydrate as well as its amorphous or crystalline structure. The water release typically begins at 130–150 °C, while significant decomposition is found starting at 250–350 °C (Kurnakow and Rode 1928). The mean rotational and translational temperatures within the argon plasma are 177 and 192 °C for the 1000 mbar and 100 mbar atmospheres, respectively. Since these are only mean temperatures, the temporary local temperatures within streamers might well exceed the given hydrate decomposition temperatures.

The calculated rotational temperatures would not necessarily be equal to or representative for the corresponding gas kinetic temperatures at 100 mbar, while this certainly is true at 1000 mbar as proven by Machala *et al* (2007). Since the interactions between the gas particles are declining with decreasing gas densities, the rotational temperature and the gas kinetic temperature should differ below a certain pressure. However, it was shown by other groups (e.g. Goyette *et al* 1996) that for many gas discharges, $T_{rot} = T_{gas}$ is still valid at pressures of 27 mbar and maybe below. While the rotational temperature of the gas remained near room temperature during the plasma treatment of air at atmospheric pressure, elevated rotational temperatures of 87, 92 and 112 °C were produced by the 100 mbar air plasma, the 1000 mbar nitrogen plasma and the 100 mbar nitrogen plasma, respectively. The argon plasma discharges reached significantly higher rotational temperatures of 177 °C at a pressure of 1000 mbar and 192 °C at 100 mbar (cf table 2). The collisional quenching of excited nitrogen states in air should lead to an enhanced energy transfer from electronic states into vibronic states and thus generate higher rotational and vibrational temperatures for the air discharges compared to discharges in nitrogen. However, the effect of the oxygen content within nitrogen discharges is not limited to the quenching of metastables, but would also include

- faster microdischarge decay times,
- shorter discharge durations,
- lower transferred charges per microdischarge and
- increasing streamer diameters

upon increasing oxygen content (Höft *et al* 2013). All of these effects should on one hand lead to a decrease in transferred energy per HV pulse as well as in energy densities within the plasma. On the other hand, higher breakdown levels and thus higher reduced electric fields during the ignition of the plasma would be expected. Even though the overall effects leading to rotational, vibrational and electron temperatures as well as the reduced electric fields given in table 2 cannot be fully accounted and described by the chosen analytical methods, the opposing effects as described by Höft *et al* (2013) might well explain the presented results, even though these are contrary to the usual expectation. This also applies to the electron temperatures, which are usually expected to be reduced upon increasing pressures, while the calculated mean electron temperatures (cf table 2) were found to be reduced for the presented setup.

Fixing the sacrificial electrode, i.e. disabling the electrode cleaning device resulted in a much smaller release of water during the plasma conditioning process. Without cleaning the surface, a much thicker film of reaction products should form, which would typically exhibit large porosities. A decreased water release due to an increased effective surface area and an increased passivation film thickness would fit well to the assumption of decomposing hydrates due to the elevated rotational and vibrational temperatures. The increased reduction rates of CO_2 and CO without cleaning device might originate in the use of stainless steel as sorbent, i.e. as sacrificial electrode. Without the cleaning device, the passivating chromium layer is broken after a distinct plasma treatment time. If the cleaning device is turned on, the amorphous adfilm gets permanently removed and thus the sacrificial electrode should always be covered by an intact Cr_2O_3 passivation layer. The exact chemical composition of the adfilm and the development of it during the plasma treatment time has not been evaluated, yet. Thus, all these assumptions on the underlying processes are speculative, of course, while some processes are completely unclear, e.g. the decreased reduction rate of

nitrogen contaminants from argon while the cleaning device is turned off.

The determined electron temperatures are proximate to the known dissociation maximum for oxygen within gaseous mixtures of nitrogen and oxygen (cf Penetrante *et al* 1997), thus this plasma discharge should be most effective for the removal of oxygen from the gas phase via chemical reactions with the sorbent material. Even though the breakdown voltages after the Paschen law in the present cases should get reduced similar to the pressure (Hess 1976), the reduced electric field should be slightly reduced at higher pressures (Holzer 2003). Thus, the electron temperatures should slightly decrease upon increasing pressures, which did not take place according to the presented results.

The comparison of results for the same gases at different pressures doesn't reveal any significant differences. Varying the pressures causes different gas and electron temperatures, different reduced field strength and different gas particle densities. A reduction of the particle density would certainly lead to a similarly reduced collision rate between gas particles and the electrode's surface and thus the formation of the adsorbate film should be slowed down accordingly. However, this did not take place during any of the experiments described above. Therefore, the passivating adsorbate film seems to be the determing factor of the gas purification pace, hence the cleaning of the rotating electrode by means of a brush appears to be insufficient for an effective gas purification device. Therefore, the approach should be modified in order to avoid the necessity of device cleaning by using a sorbent powder instead of a massive sacrificial electrode. This would enlarge the surface to bulk ratio to such an extent that an adfilm removal should be obsolete and make use of the increased reduction rates of carbon oxides found during the experiment without cleaning device. Furthermore, different, less expensive materials might be used for specific applications, e.g. silicon nitride for the purification of nitrogen, which would not only remove oxygen, but also release additional nitrogen for each chemisorbed oxygen molecule (cf Dahle *et al* 2013).

5. Summary

A setup for the purification of inert gases using a DBD plasma together with a rotating sacrificial electrode with an attached electrode cleaning system to enhance the capacity and reaction rates was presented. The setup has been found to be ineffective for the removal of high contents of contaminants despite the electrode cleaning device. A purification of medium purity nitrogen gas using this approach was shown to be quite successful. Due to the small reaction rates, a different setup employing powder sorbents was proposed. The conditioning of technical argon by the rotating sacrificial electrode DBD setup was able to remove oxygen and nitrogen, while the water content increased during the plasma treatment. This effect was discussed taking into account the rotational temperatures, which were determined to be well beyond 150 °C.

Acknowledgments

We thankfully acknowledge the technical assistance of Aaron L Arendt.

References

Avramidis G, Klarhöfer L, Maus-Friedrichs W, Militz H and Viöl W 2012 Influence of air plasma treatment at atmospheric pressure on wood extractives *Polym. Degrad. Stab.* **97** 469–71

Baker J D, Meikrantz D H and Tuggle D G 1997 Method for the purification of noble gases, nitrogen and hydrogen *US Patent* 5669961 A

Bauer H, Becker H and Scholz W 1988 Gas stream purification process by nitrogen washing *European Patent* 0256413 A3

Bergman T J, Howell J K, Markowski M L, Natwora J P Jr and Thompson D R 1999 Cryogenic system for producing ultra-high purity nitrogen *European Patent* 0916383 A1

Bligh B R and Godber S J 1980 Method of purifying crude argon *European Patent* 0006320 A1

Boveri G, Ghisolfi G and Giordano D 1995 Process for the purification of inert gases *European Patent* 0660746A1

Campbell M J 1990 Membrane process and system for nitrogen production *US Patent* 4960579 A

Dahle S, Gustus R, Viöl W and Maus-Friedrichs W 2012 DBD plasma treatment of titanium in O2, N2 and air *Plasma Chem. Plasma Process.* **32** 1109–25

Dahle S, Wegewitz L, Qi F, Weber A and Maus-Friedrichs W 2013 Silicon dioxide coating of titanium dioxide nanoparticles from dieletric barrier discharge in a gaseous mixture of silane and nitrogen *Plasma Chem. Plasma Proccess.* **33** 839–53

DeMarco S S 1967 Purification of nitrogen which contains methane *US Patent* 3507127 A

El-Mahdy G A, Atta A M, Hegazy M M, Eissa M M, Fathy M M, Sayed F M, Dyab A K F and Al-Lohedan H 2012 Microscopic studies on the corrosion resistance of reinforced carbon steel *Int. J. Electrochem. Sci.* **7** 8597–611

Fantz U 2006 Basics of plasma spectroscopy *Plasma Sources Sci. Technol.* **15** S137–47

Gajula S R, Dongara R, Pavagada R C, Konda R K, Halgeri B A, Singaram M and Singh S 2009 Oxidation catalyst for the purification of nitrogen gas containing organic impurities *European Patent* 2019730 A1

Goyette A N, Jameson W B, Anderson L W and Lawler J E 1996 An experimental comparison of rotational temperature and gas kinetic temperature in a H2 discharge *J. Phys. D: Appl. Phys.* **29** 1197–201

Guldberg C M and Waage P 1879 Concerning chemical affinity erdmann's *J. für Praktische Chemie* **127** 69–114

Greter L and Venet F 2003 Cryogenic air separation process and apparatus *European Patent* 0935109 B1

Hagelaar G J M and Pitchford L C 2005 Solving the Boltzmann equation to obtain electron transport coefficients and rate coefficients for fluid models *Plasma Sources Sci. Technol.* **14** 722–33

Hess H 1976 *Der elektrische Durchschlag in Gasen* (Berlin: Akademie-Verlag)

Hirschberg J, Omairi T, Mertens N, Helmke A, Emmert S and Viöl W 2013 Influence of excitation pulse duration of dielectric barrier discharges on biomedical applications *J. Phys. D: Appl. Phys.* **46** 165201

Höft H, Kettlitz M, Hoder T, Weltmann K D and Brandenburg R 2013 The influence of O2 content on the spatio-temporal development of pulsed driven dielectric barrier discharges in O2/N2 gas mixtures *J. Phys. D: Appl. Phys.* **46** 095202

Holzer F 2003 Oxidation von organischen Verbindungen unter Nutzung von porösen und unporösen

Feststoffen im nichtthermischen Plasma *PhD thesis* urn:nbn:de:gbv:3-000006279
Hsiung T H-L and Wallace J B Jr 1999 Bulk nitrogen purification process that requires no hydrogen in the regeneration *US Patent* 5993760 A
Jain R 1994 Production of nitrogen *European Patent* 0590946 A1
Jain R and Tseng J K 1998 Inert gas purification *European Patent* 0832678 A3
Kamrath D J 1990 Generation and purification of nitrogen *European Patent* 0407136 B1
Koichi c/o Japan Pionics Co. Ltd. Kitahara, Kenji c/o Japan Pionics Co. Ltd. Ohtsuka, Noboru c/o Japan Pionics Co. Ltd. Takemasa, Shinobu c/o Japan Pionics Co. Ltd. Kamiyama 1997 Process for purification of rare gas *European Patent* 0475312 B1
Kurnakow N S and Rode E J 1928 Chemische Konstitution der natürlichen eisenoxidhydrate *Chem. Constitution Nat. Iron Oxide Hydrates—Phys. Chem. Anal. Hydrate Forms* **169** 57–80
Lane J A, Bonaquist D P, Shreiber E and Arman B 2009 Gas stream purification method *European Patent* 1880155 A2
Laux C O 2002 Radiation and nonequilibrium collisional-radiative models *Physico-Chemical Modeling of High Enthalpy and Plasma Flows* ed D Fletcher *et al* (*Karman Institute Lecture Series 2002–07*) (Rhode-Saint-Genèse, Belgium: Karman Institute)
Laux C O 2003 Optical diagnostics of atmospheric pressure air plasma *Plasma Sources Sci. Technol.* **12** 125–38
Lawless W N 2001 Nitrogen purification device *US Patent* 6290757 B1
Lide D R 1998 *CRC Handbook of Chemistry and Physics* (Florida, FL: CRC Press) LLC, ISBN 0-8493-0479-2
Machala Z, Janda M, Hensel K, Jedlovsky I, Lestinska L, Foltin V, Martisovits V and Morvova M 2007 Emission spectroscopy of atmospheric pressure plasmas for bio-medical and environmental applications *J. Mol. Spectrosc.* **243** 194–201
Mallett M W 1950 Purification of argon *Ind. Eng. Chem.* **42** 2095–6
Newton A S 1949 Nitrogen purification process *US Patent* 2487360 A
Paris P, Aints M, Valk F, Plank T, Haljaste A, Kozlov K V and Wagner H-E 2005 Intensity ratio of spectral bands of nitrogen as a measure of electric field strength in plasmas *J. Phys. D: Appl. Phys.* **38** 3894–9
Penetrante B M, Hsiao M C, Bardsley J N, Merritt B T, Vogtlin G E, Kuthi A, Burkhart C P and Bayless J R 1997 Identification of mechanisms for decomposition of air pollutants by non-thermal plasma processing *Plasma Sources Sci. Technol.* **6** 251–9
Reich M and Kapenekas H 1957 Nitrogen purification *Ind. Eng. Chem.* **49** 869–73
Rodt V 1930 Yellow iron oxide hydrate and its connnection with rust and iron ore *Naturwissenschaften* **18** 230–1
Schah M S, Khan N and Ahmad R 2009 Characterization and effect of argon–nitrogen plasma on nitridation of aluminum alloy *J. Nat. Sci. Math.* **49** 1–17
Song M A, Lee Y W and Chung T H 2011 *Phys. Plasmas* **18** 023504
Staak D, Farouk B, Gutsol A and Fridman A 2005 Characterization of a dc atmospheric pressure normal glow discharge *Plasma Sources Sci. Technol.* **14** 700–11
Takao A, Takashi E and Shinichi I 1969 Method for removal of impurities in rare gases *US Patent* 3467493 A
Wegewitz L, Dahle S, Höfft O, Voigts F, Viöl W, Endres F and Maus-Friedrichs W 2011 Plasma-oxidation of Ge(1 0 0) surfaces using a dielectric barrier discharge investigated by MIES, UPS and XPS *J. Appl. Phys.* **110** 033302
Yamamoto T and Yamashita N 2001 Method and apparatus for purification of argon *European Patent* 0956928 A4
Yao J, Chen J J and Elliot D G 1986 Method and apparatus for purification of high nitrogen content gas *European Patent* 0195593 B1